

Internal Compact Dual-Band Printed Loop Antenna for Mobile Phone Application

Yun-Wen Chi and Kin-Lu Wong

Abstract—A novel dual-band printed loop antenna very promising for application in mobile phones as an internal antenna is presented. The antenna comprises an outer loop strip and an inner inverted-L strip connected to and enclosed by the outer loop strip. The antenna occupies a compact area of $15 \times 50 \text{ mm}^2$ only, yet generating three resonant modes to form two wide bands at about 900 and 1800 MHz for the Global System for Mobile Communication/Digital Communication System operation. Detailed design considerations of the three excited modes are described in the paper. When a shielding metal case is placed close to the antenna, small effects on the antenna's impedance matching are seen, allowing compact integration of the antenna with nearby conducting elements or electronic components. The antenna is also found to result in small excited surface current distributions on the system ground plane of the mobile phone. This behavior is expected to lead to reduced user's hand effects on the radiation efficiency of the antenna.

Index Terms—Dual-band antennas, mobile phone antennas, printed antennas, printed loop antennas.

I. INTRODUCTION

Conventional internal antennas for mobile phone applications are generally in the forms of the planar inverted-F patch antenna, very-low-profile printed or metal-plate monopole antenna, and so on [1]. Such internal mobile phone antennas usually excite large surface currents on the system ground plane of the mobile phone, which functions as an effective radiation portion, especially for the lower frequency operation in the Global System for Mobile Communication (GSM, 890 ~ 960 MHz) band. Owing to the large excited surface currents on the system ground plane, especially in the region near the internal antenna, an isolation distance of about 7 mm or larger between the antenna and the nearby conducting elements or electronic components in the mobile phone is usually required to avoid large degradation effects on the performances of the internal antenna [2], [3].

To decrease or eliminate the system ground plane effects on the antenna performances, the modified one-wavelength loop antenna has been proposed [4]. This kind of modified loop antenna is expected to operate as a self-balanced structure, thus resulting in small excited surface currents on the system ground plane. However, owing to its one-wavelength resonant structure, such a modified loop antenna is usually bulky in volume, causing a limitation in its practical application for mobile phones. In this paper, we present a novel printed loop antenna for mobile phone applications. The antenna has a planar configuration and is easy to implement with a low cost by printing on the system circuit board of the mobile phone. In addition, the antenna occupies a compact area of $15 \times 50 \text{ mm}^2$ only, yet providing two wide bands for GSM and Digital Communication System (DCS, 1710 ~ 1880 MHz) operation.

The antenna comprises an outer loop strip and an inner inverted-L strip, and provides two resonant loop paths. The first loop path is controlled by the outer loop strip, while the second loop path is formed by the inner inverted-L strip and part of the outer loop strip. The two loop paths support three resonant modes for the antenna. The first and second modes are formed into a wide band at about 1 GHz to easily

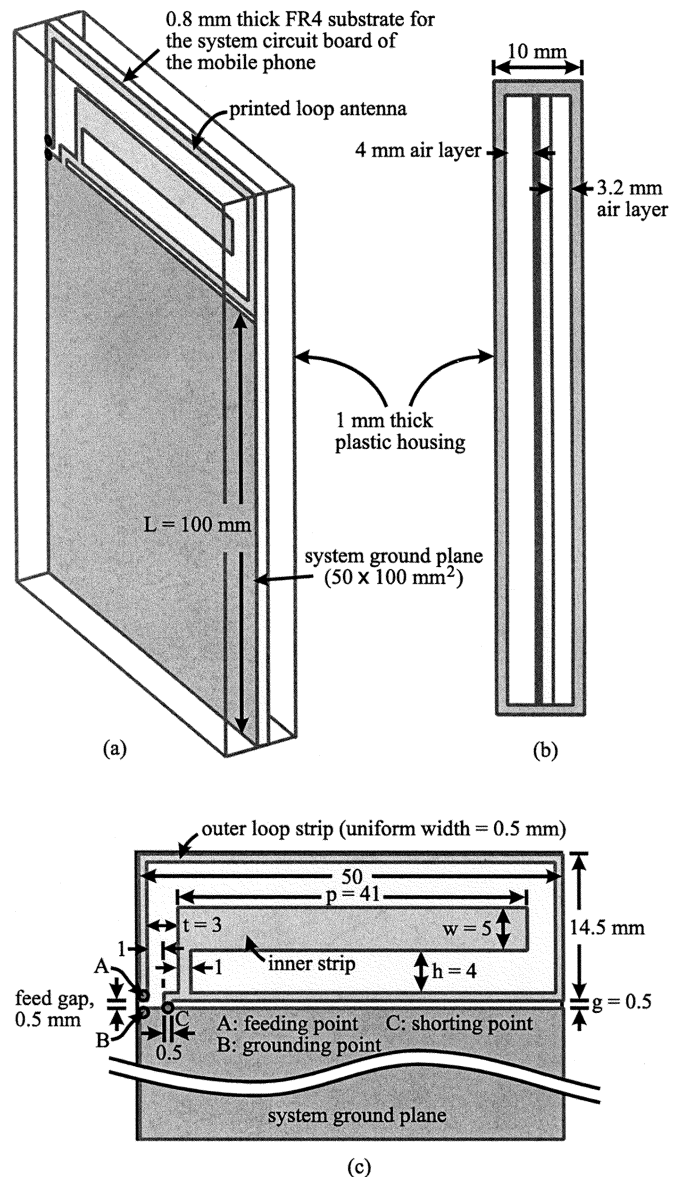


Fig. 1. (a) Geometry of the printed loop antenna enclosed by the housing of the mobile phone. (b) Side view of (a). (c) Detailed dimensions of the antenna.

cover the GSM operation, and the third mode provides a wide band at about 1800 MHz to cover the DCS operation.

The antenna can lead to small excited surface current distributions on the system ground plane. This behavior is expected to result in a small isolation distance required between the antenna and the nearby conducting elements or electronic components in the mobile phone. For this verification, effects of a shielding metal case placed close to the antenna are studied. In addition, it may also be expected that the user's hand effects will become small, when the excited surface current distributions on the system ground plane are small. For this analysis, the study of the antenna with the user's hand is conducted.

II. DESIGN CONSIDERATIONS OF PROPOSED ANTENNA

Fig. 1(a) shows the geometry of the antenna enclosed by the housing of the mobile phone, and the side view of the geometry is shown in Fig. 1(b). The mobile phone housing is fabricated using a 1-mm thick acrylonitrile butadiene styrene (ABS) plate with relative permittivity

Manuscript received August 6, 2006; revised November 14, 2006.

The authors are with the Department of Electrical Engineering, National Sun Yat-Sen University, Kaohsiung 804, Taiwan, R.O.C.

Digital Object Identifier 10.1109/TAP.2007.895641

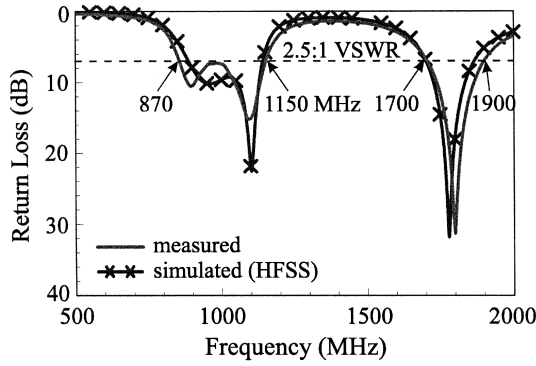


Fig. 2. Measured and simulated (HFSS) return loss.

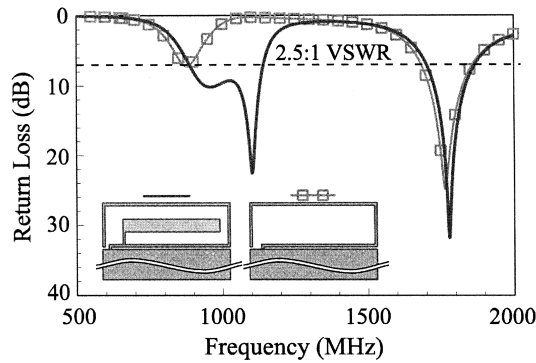


Fig. 3. Comparison of the simulated (HFSS) return loss for the antenna studied in Fig. 2 and the case without the inner inverted-L strip (see the inset in the figure).

(ϵ_r) 3.5 and conductivity (σ) 0.02 S/m. The ABS is a practical material for the housing of general mobile phones. The housing can avoid direct contact of the user's hand with the antenna and the system ground plane in the experiment.

The antenna is printed on the top ungrounded portion (size $50 \times 15 \text{ mm}^2$) of a 0.8-mm thick FR4 substrate, which is considered as the system circuit board of the mobile phone. On the front side of the FR4 substrate, a ground plane of width 50 mm and length (L) 100 mm is printed. The effect of different ground plane lengths was studied, and results are shown in Fig. 8.

The preferred design dimensions of the antenna are presented in Fig. 1(c). The antenna comprises an outer loop strip of uniform width 0.5 mm and an inner inverted-L strip. The outer loop strip generally follows the boundary of the ungrounded portion, with a small gap (g) of 0.5 mm to the top edge of the system ground plane. By choosing a small value of g , good impedance matching of the antenna can be achieved. Detailed effects of the gap g are discussed in Fig. 7. Note that one end of the outer loop strip is the antenna's feeding point (point A), and the other end is short-circuited to the system ground plane, with the shorting point (point C) having a small distance to point A as shown in the figure. The antenna has a 0.5-mm feed gap across point A and the top edge of the system ground plane. To test the antenna in the experiment, a 50- Ω mini coaxial line is used, with its central conductor connected to point A and its outer grounding sheath connected to point B, the grounding point.

The total length of the outer loop strip is 128 mm, about 0.77 wavelength of the frequency at 1800 MHz. Owing to the presence of the FR4 substrate, which decreases the resonant length of the antenna's possible modes, the outer loop strip provides a first loop path (see the loop paths shown in Fig. 4) supporting a 0.5-wavelength loop mode at

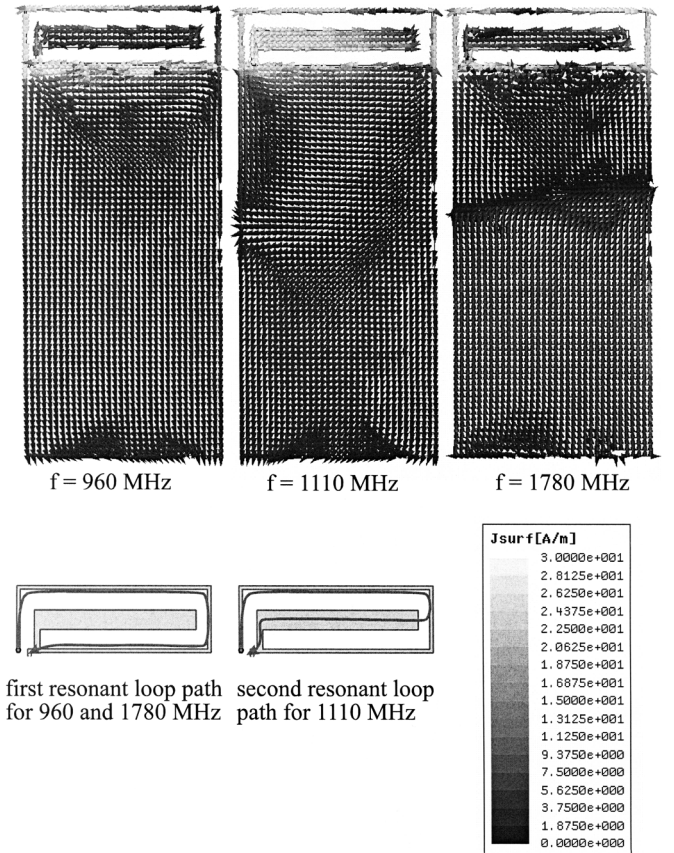


Fig. 4. Simulated (HFSS) excited surface current distributions at 960, 1110, and 1780 MHz for the antenna studied in Fig. 2.

about 900 MHz for GSM operation and a 1.0-wavelength loop mode at about 1800 MHz for DCS operation. However, when the inner inverted-L strip is not present, the excited 0.5-wavelength loop mode cannot be successfully excited with acceptable impedance matching. These two loop modes contributed by the outer loop strip are denoted as the first and third modes of the antenna.

The inner inverted-L strip consists of a long horizontal arm and a short vertical arm. The horizontal arm is of length (p) 41 mm and width (w) 5 mm. Through the vertical arm of width 1 mm and length (h) 4 mm, which has a distance (t) of 3 mm to the outer loop strip, the inner strip is connected to the outer loop strip near the shorting point at point C. This inner inverted-L strip and part of the outer loop strip provides a second loop path (see Fig. 4) supporting a 0.5-wavelength loop mode (the antenna's second mode), which is excited at adjacent frequencies to the antenna's first mode and also helps improve the impedance matching of the first mode. The antenna's first and second modes are formed into a wide band centered at about 1 GHz to easily cover the GSM operation. Good impedance matching of the antenna's lower band formed by the first and second modes was found to be strongly affected by the parameters p , w , t , and h related to the inner inverted-L strip. Their detailed effects are discussed in Figs. 5 and 6.

III. RESULTS OF THE PROPOSED ANTENNA

Fig. 2 shows the measured and simulated return loss of the constructed prototype. The simulated results are obtained using Ansoft simulation software High Frequency Structure Simulator (HFSS) [5], and good agreement between the measurement and simulation is seen. As expected, three resonant modes with good impedance matching are

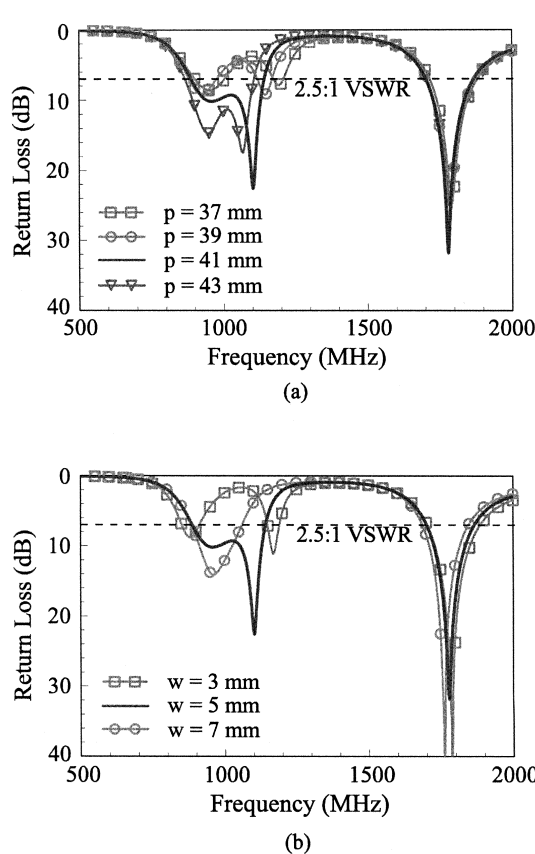


Fig. 5. Simulated (HFSS) return loss as a function of (a) p and (b) w . Other dimensions are the same as studied in Fig. 2.

excited. The first and second modes are formed into a wide band with a bandwidth as large as 280 MHz (870 ~ 1150 MHz), which makes it easy to cover the GSM operation. The third mode has a bandwidth of 200 MHz (1700 ~ 1900 MHz), also satisfying the required bandwidth for DCS operation. The bandwidth definition used here is 2.5:1 VSWR, which is a higher standard for practical mobile phone applications, because the internal antennas of general mobile phones are usually designed based on the bandwidth definition of 6 dB return loss (3:1 VSWR) or even less.

Fig. 3 shows the comparison of the simulated return loss for the antenna studied in Fig. 2 and the case without the inner inverted-L strip. When the inner strip is not present, there are only two modes (the antenna's first and third modes) excited. In addition, only the third mode at about 1800 MHz is excited with good impedance matching; the first mode is not excited with acceptable impedance matching, making it not capable of covering the whole GSM band. Conversely, with the presence of the inner inverted-L strip, an additional mode (the antenna's second mode) is excited with good impedance matching, and the impedance matching of the first mode is also greatly improved. This characteristic leads to a wide band for GSM operation. The presence of the inner strip also shows very small effects on the antenna's third mode for DCS operation.

Fig. 4 shows the simulated surface current distributions at the resonant frequencies (960, 1110, and 1780 MHz) of the antenna's three excited modes. For all the three frequencies, there are small excited surface current distributions on the system ground plane. For $f = 960$ and 1780 MHz, the excited surface currents indicate that the first and third modes are controlled by the outer loop strip, which is denoted as the antenna's first loop path. Furthermore, the first and third modes

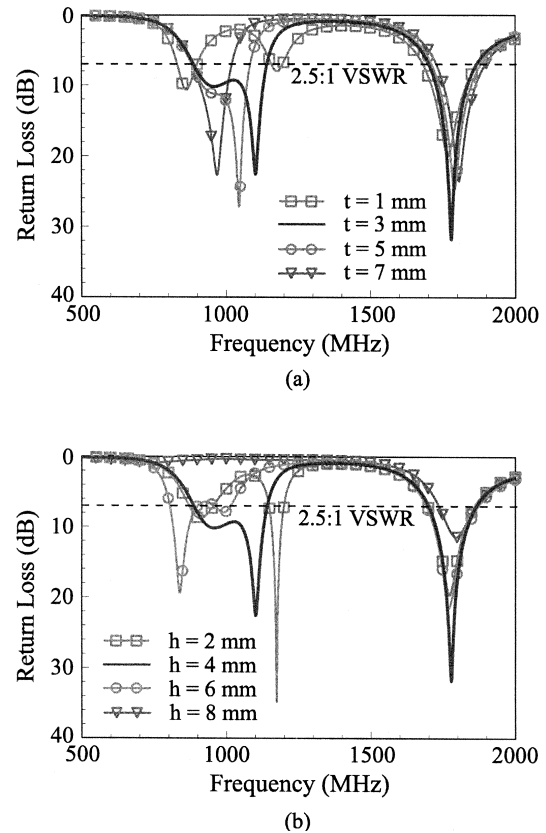


Fig. 6. Simulated (HFSS) return loss as a function of (a) t and (b) h . Other dimensions are the same as studied in Fig. 2.

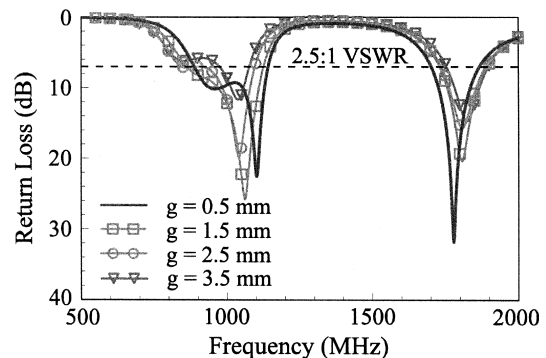


Fig. 7. Simulated (HFSS) return loss as a function of g , the gap between the outer loop strip and system ground plane. Other dimensions are the same as studied in Fig. 2.

can be considered as the 0.5-wavelength and 1.0-wavelength modes of this first loop path. The excited surface currents at 1110 MHz suggest that a second loop path is created, which is formed by the inner inverted-L strip and part of the outer loop strip as indicated in the figure and leads to the excitation of the antenna's second mode. This second mode can be considered as the 0.5-wavelength mode of the second loop path. Although the first and third modes do not appear to be balanced modes, their loop structures are still very likely to provide a closed current path for the excited surface currents. This may lead to smaller excited surface current distributions on the system ground plane, compared to the conventional monopole mobile phone antenna. In addition, the results indicate that large excited surface current distributions on the system ground plane are seen only in the ground plane portion very

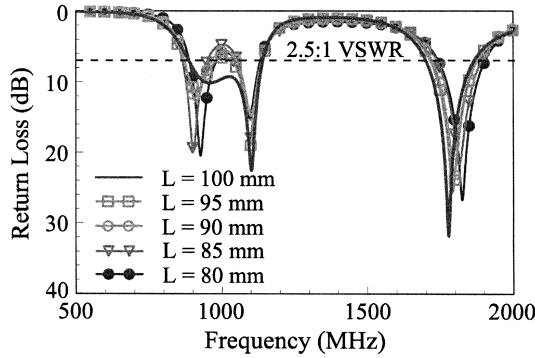


Fig. 8. Simulated (HFSS) return loss as a function of L , the length of the system ground plane. Other dimensions are the same as studied in Fig. 2.

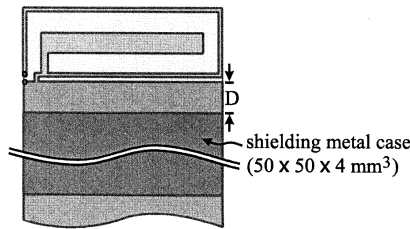
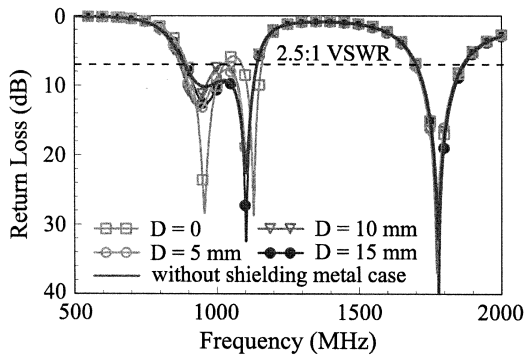


Fig. 9. Simulated (HFSS) return loss as a function of D , the distance between the shielding metal case and the antenna. Other dimensions are the same as studied in Fig. 2.

near the printed slot, while those of the conventional monopole mobile phone antenna are seen over a larger portion on the system ground plane (not shown here for brevity).

A. Parametric Study for the Antenna

To demonstrate the effects of the dimensions (p and w) and location (t and h) of the inner inverted-L strip, a parametric study is conducted. Fig. 5 shows the simulated return loss as a function of p and w , respectively. In Fig. 5(a), the results for the parameter p varied from 37 to 43 mm are shown. The antenna's third mode at about 1800 MHz is almost not affected by the parameter p . Conversely, with a larger value of p , the resonant frequency of the antenna's second mode is shifted to lower frequencies and is closer to that of the first mode, and the impedance matching of the first mode is also improved. This behavior is largely because when p is increased, the open end of the inner inverted-L strip will be much closer to the outer loop strip, which may lead to a better formation of the additional second loop path for the antenna. In this case, successful excitation of the antenna's first and second modes can be achieved. Results for the parameter w varied from 3 to 7 mm are presented in Fig. 5(b). Similarly, small effects on the antenna's third

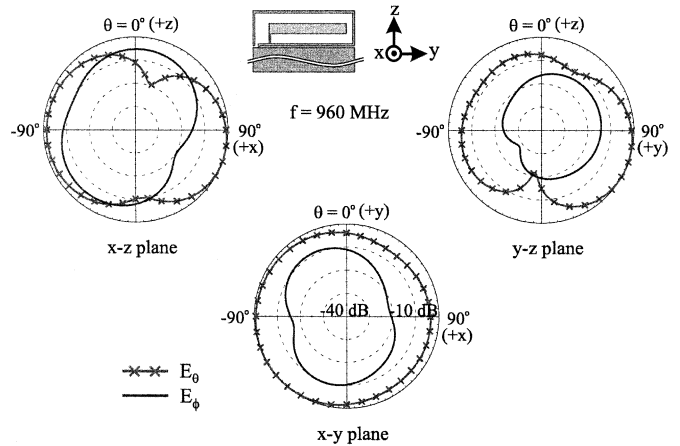


Fig. 10. Measured radiation patterns at 960 MHz for the antenna studied in Fig. 2.

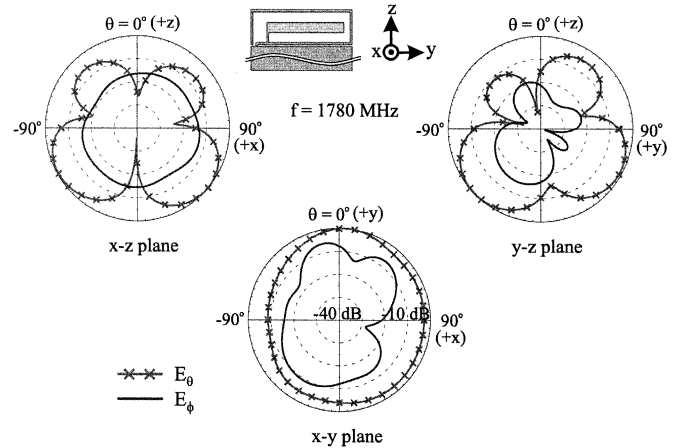


Fig. 11. Measured radiation patterns at 1780 MHz for the antenna studied in Fig. 2.

mode are seen, and there are large effects on the antenna's first and second modes. This may be explained that a larger width of the inner inverted-L strip (that is, w is larger) can lead to some variations in the coupling between the open end of the inner inverted-L strip and the outer loop strip, which may in turn cause some variations in the effective path length of the additional second loop path described in Fig. 4. Thus, the resonant frequency of the second mode can also be controlled by the width w , and for achieving a wider bandwidth for the antenna's lower band, the width w is selected to be 5 mm for the preferred dimension in this study.

Effects of the location of the inner inverted-L strip are analyzed in Fig. 6, in which the simulated return loss as a function of t and h are presented. In Fig. 6(a), results for the parameter t varied from 1 to 7 mm are shown. Again, small effects on the antenna's third mode are seen. When a proper value of t is chosen, the antenna's first and second modes can be excited at adjacent frequencies to form a wide band. From the results, the value of t was selected to be 3 mm for the preferred design in this study. For the effects of h shown in Fig. 6(b), when h is too large ($h = 8$ mm), the antenna's third mode is greatly affected, and both of the antenna's first and second modes can no longer be excited. This behavior is largely because, for larger values of h , the inner inverted-L strip will be too close to the outer loop strip, which causes destructive coupling effects for the antenna. From the results for various values of h , the preferred value of h was chosen to be 4 mm.

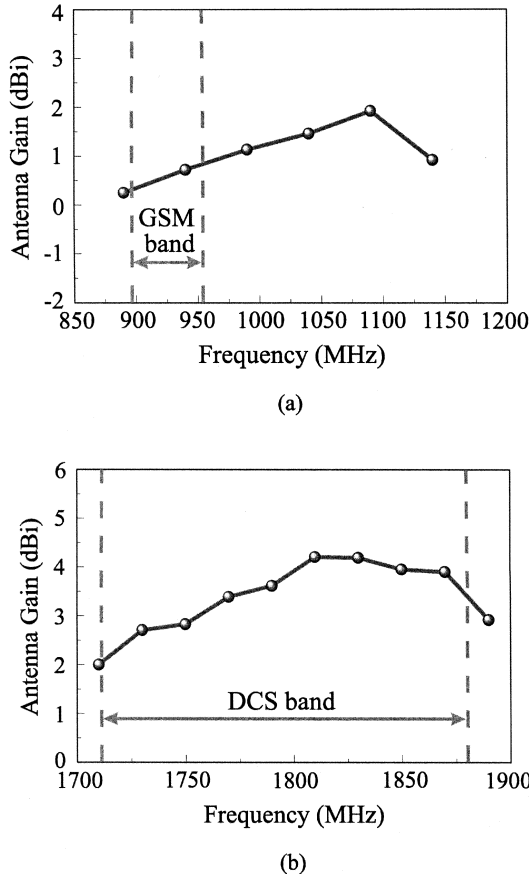


Fig. 12. Measured antenna gain for the antenna studied in Fig. 2. (a) Lower band. (b) Upper band.

Fig. 7 shows the simulated return loss as a function of g , the gap between the outer loop strip and system ground plane. Results indicate that the parameter g affects all the antenna's three modes. In order to achieve good impedance matching for the three modes, the value of g should be selected to be small. Thus, the value of g was selected to be 0.5 mm only.

Effects of the ground-plane length L are also studied. Fig. 8 shows the simulated return loss for L varied from 100 to 80 mm. The obtained bandwidths for the antenna's lower band are in general about the same, except for the small frequency range at about 1 GHz in which the return loss is still better than about 5 dB. For the antenna's upper band or the third mode, only some slight frequency shifting is observed. The results suggest that the ground plane length L has small effects on the achievable bandwidths of the antenna, which is quite different from those observed for the conventional internal patch antenna for mobile phones [6], [7]. With this attractive feature, the antenna can be applied to the mobile phone with various possible ground plane lengths.

Fig. 9 presents the simulated return loss for the antenna with the shielding metal case, whose distance to the antenna is denoted as D . The metal case can provide a coupling-free space for accommodating nearby electronic components in the mobile phone. From the results, almost no variations in the impedance matching of the third mode are seen for D varied from 15 to 0 mm. For the first and second modes, small variations are observed. These results suggest that compact integration of the antenna with nearby elements can be obtained. This property is similar to that of the EM compatible (EMC) internal patch antenna having a vertical ground wall [8]–[11] for achieving the same behavior as obtained here.

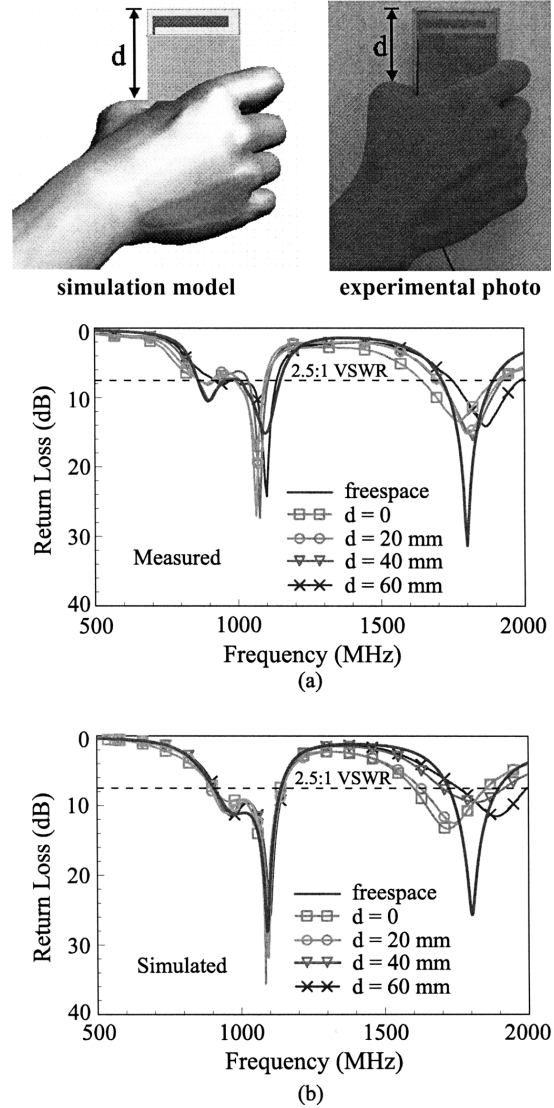


Fig. 13. (a) Measured and (b) simulated (SEMCAD) return loss for $d = 0, 20, 40$, and 60 mm for the antenna studied in Fig. 2 with the user's hand.

B. Radiation Characteristics for the Antenna

Figs. 10 and 11 plot the measured radiation patterns at 960 and 1780 MHz (center frequencies of the antenna's first and third modes). The radiation patterns at 1110 MHz (center frequency of the antenna's second mode) are seen to be close to those at 960 MHz shown in Fig. 10, and are thus not shown here for brevity. Monopole-like radiation patterns at 960 MHz are seen, and omnidirectional radiation in the azimuthal plane (x - y plane) is generally observed. For the radiation patterns at 1780 MHz shown in Fig. 12, more variations and nulls in the patterns are seen. These patterns are in general similar to those observed for the conventional internal mobile phone antennas [1]. Fig. 12 presents the measured antenna gain. For frequencies over the GSM band, the antenna gain is about $0.3 \sim 0.8$ dBi, while that for the DCS band ranges from about 2.0 to 4.2 dBi.

IV. USER'S HAND EFFECTS ON ANTENNA PERFORMANCES

The experimental photo and simulation model for the study of the user's hand effects are shown in Fig. 13. The parameter d denotes the distance from the top edge of the mobile phone to the top of the user's thumb portion. The simulation hand model is provided by SPEAG

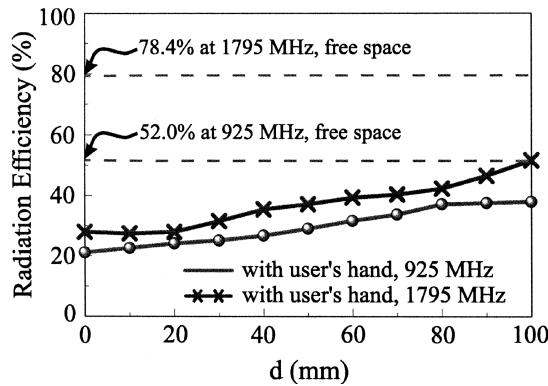


Fig. 14. Simulated radiation efficiency (SEMCAD) as a function of d for the antenna studied in Fig. 2 with the user's hand.

simulation software SEMCAD [12], and the hand model comprises the skin, muscle, and bones, whose relative permittivity and conductivity at the studied frequencies are obtained from [13]. For the antenna studied in Fig. 2 with the presence of the user's hand, the measured and simulated return loss for d varied from 0 to 60 mm are shown in Fig. 13(a) and (b), respectively. Good agreement between the measurement and simulation is generally obtained.

Fig. 14 shows the simulated radiation efficiency as a function of d . The frequencies at 925 and 1795 MHz, center frequencies of the GSM and DCS bands, are studied. Results show that the radiation efficiency is decreased with a decrease in d . However, for the worst case of $d = 0$, the radiation efficiency is still about 20% at 925 MHz and about 28% at 1795 MHz. The results are better than those of the internal patch antenna with the user's hand [14], in which the radiation efficiency is only about 9.1% at 925 MHz and 18.4% at 1795 MHz for the condition with $d = 0$.

The simulated three-dimensional radiation patterns obtained from SEMCAD at 925 and 1795 MHz are also studied. It is observed that the radiation power is greatly absorbed by the user's hand in the forearm direction, leading to large distortions in the antenna's radiation patterns. Much larger pattern distortions are seen when the distance d is smaller, especially for the results at 1795 MHz. The results indicate that the radiation patterns of the antenna are strongly dependent on the parameter d , which is similar to those observed for the internal patch antenna [14].

V. CONCLUSION

A novel internal dual-band printed loop antenna suitable for mobile phone application has been proposed and studied. The antenna has a planar structure with a simple metal strip pattern, making it easy to fabricate with a low cost. A preferred design occupying a compact area of $15 \times 50 \text{ mm}^2$ has been implemented and tested. The antenna can generate three modes to form two wide bands at about 900 and 1800 MHz for GSM/DCS operation. A parametric study has been conducted, and design considerations for selecting the preferred design dimensions have been discussed. The bandwidth of the antenna has been found to be insensitive to the variations in the ground plane length of the mobile phone, which makes the antenna very attractive to be applied in the mobile phones with various possible ground plane lengths.

The antenna also showed similar EMC property as the internal patch antennas with a vertical ground wall that have been recently reported [8]–[11]. This feature allows the nearby conducting elements or electronic components in the mobile phone to be placed very close to the antenna to achieve a compact integration. In addition, results have shown

that with the presence of the user's hand, the radiation efficiency of the antenna is better than that of the internal patch antenna. However, large distortions in the radiation patterns owing to the presence of the user's hand are still observed, which is similar to that of the internal patch antenna.

REFERENCES

- [1] K. L. Wong, *Planar Antennas for Wireless Communications*. New York: Wiley, 2003.
- [2] K. L. Wong, S. W. Su, C. L. Tang, and S. H. Yeh, "Internal shorted patch antenna for a UMTS folder-type mobile phone," *IEEE Trans. Antennas Propag.*, vol. 53, pp. 3391–3394, Oct. 2005.
- [3] S. W. Su, K. L. Wong, C. L. Tang, and S. H. Yeh, "Wideband monopole antenna integrated within the front-end module package," *IEEE Trans. Antennas Propag.*, vol. 54, pp. 1888–1891, Jun. 2006.
- [4] H. Morishita, Y. Kim, and K. Fujimoto, "Design concept of antennas for small mobile terminals and the future perspective," *IEEE Antennas Propag. Mag.*, vol. 44, pp. 30–43, 2002.
- [5] Ansoft Corporation HFSS [Online]. Available: <http://www.ansoft.com/products/hf/hfss/>
- [6] T. Y. Wu and K. L. Wong, "On the impedance bandwidth of a planar inverted-F antenna for mobile handsets," *Microw. Opt. Technol. Lett.*, vol. 32, pp. 249–251, Feb. 2002.
- [7] P. Vainikainen, J. Ollikainen, O. Kivekas, and I. Kelder, "Resonator-based analysis of the combination of mobile handset antenna and chassis," *IEEE Trans. Antennas Propag.*, vol. 50, pp. 1433–1444, 2002.
- [8] C. M. Su, K. L. Wong, C. L. Tang, and S. H. Yeh, "EMC internal patch antenna for UMTS operation in a mobile device," *IEEE Trans. Antennas Propag.*, vol. 53, pp. 3836–3839, Nov. 2005.
- [9] K. L. Wong and C. H. Chang, "Surface-mountable EMC monopole chip antenna for WLAN operation," *IEEE Trans. Antennas Propag.*, vol. 54, pp. 1100–1104, Apr. 2006.
- [10] K. L. Wong and C. H. Chang, "WLAN chip antenna mountable above the system ground plane of a mobile device," *IEEE Trans. Antennas Propag.*, vol. 53, pp. 3496–3499, Nov. 2005.
- [11] S. L. Chien, F. R. Hsiao, Y. C. Lin, and K. L. Wong, "Planar inverted-F antenna with a hollow shorting cylinder for mobile phone with an embedded camera," *Microw. Opt. Technol. Lett.*, vol. 41, pp. 418–419, Jun. 2004.
- [12] SEMCAD, Schmid & Partner Engineering AG (SPEAG) [Online]. Available: <http://www.semcad.com>
- [13] S. Gabriel, R. W. Lau, and C. Gabriel, "The dielectric properties of biological tissues: III. Parametric models for the dielectric spectrum of tissues," *Phys. Med. Biol.*, vol. 41, pp. 2271–2293, 1996.
- [14] C. M. Su, C. H. Wu, K. L. Wong, S. H. Yeh, and C. L. Tang, "User's hand effects on EMC internal GSM/DCS dual-band mobile phone antenna," *Microw. Opt. Technol. Lett.*, vol. 48, pp. 1563–1569, Aug. 2006.